Published in final edited form as:
Nat Immunol. 2013 December ; 14(12): 1247–1255. doi:10.1038/ni.2749.

Phosphorylation of ASC acts as a molecular switch controlling the formation of speck-like aggregates and inflammasome activity

Hideki Hara[1], **Kohsuke Tsuchiya**[1], **Ikuo Kawamura**[1], **Rendong Fang**[1], **Eduardo Hernandez-Cuellar**[1], **Yanna Shen**[1,2], **Junichiro Mizuguchi**[3], **Edina Schweighoffer**[4], **Victor Tybulewicz**[4], and **Masao Mitsuyama**[1,*]

[1]Department of Microbiology, Kyoto University Graduate School of Medicine, Yoshida konoe-cho, Sakyo-ku, Kyoto, 606-8501, Japan

[2]College of Medical Laboratory, Tianjin Medical University, Guangdong Road, Hexi District, Tianjin, 300203, China

[3]Department of Immunology and Intractable Immunology Research Center, Tokyo Medical University, 6-1-1 Shinjuku, Shinjuku-ku, Tokyo, 160-8402, Japan

[4]MRC National Institute for Medical Research, The Ridgeway, Mill Hill, London NW7 1AA, UK

Abstract

The inflammasome adaptor ASC contributes to innate immunity through the activation of caspase-1. Here we show that Syk and JNK-dependent signaling pathways are required for caspase-1 activation via the ASC-dependent inflammasomes NLRP3 and AIM2. Inhibition of Syk or JNK abolished the formation of ASC specks without affecting interaction of ASC with NLRP3. ASC was phosphorylated during inflammasome activation in a Syk- and JNK-dependent manner, suggesting that Syk and JNK are upstream of ASC phosphorylation. Moreover, phosphorylation of Tyr144 residue in mouse ASC was critical for speck formation and caspase-1 activation. These results suggested that phosphorylation of ASC controls inflammasome activity through ASC speck formation.

Inflammasomes are large multiprotein oligomers that play critical roles in host defense against microbial pathogens and the development of inflammatory disorders by facilitating the secretion of pro-inflammatory cytokines[1]. Core components of each inflammasome are pro-caspase-1 and a cytosolic pattern-recognition receptor belonging to the Nod-like receptor (NLR) family or the HIN-200 family, which contains a pyrin domain or a caspase

*Address correspondence and reprint requests to Masao Mitsuyama, Phone: +81 75 753 4441. Fax: +81 75 753 4446. mituyama@mb.med.kyoto-u.ac.jp.

AUTHOR CONRIBUTIONS

H.H. and K.T. equally contributed to the present study. H.H. initiated the study, designed and performed the macrophage and peritonitis experiments. K.T. designed and performed the HEK293 cell experiments. K.T., H.H. and M.M. wrote the manuscript; I.K. provided advice; R.F., E.H.C. and Y.S. contributed to the experiments; J.M. provided the *Mapk8*$^{-/-}$ and *Mapk9*$^{-/-}$ mice; E.S. and V.T. provided the *Syk*$^{+/+}$, *Syk*$^{+/-}$ and *Syk*$^{-/-}$ fetal liver cells; M.M. supervised the project.

Europe PMC Funders Author Manuscripts

recruitment domain (CARD). Inflammasome complexes are supposedly assembled following recognition of specific stimuli by the receptors[2,3]. Once assembled, inflammasomes serve as platforms for the activation of caspase-1, which in turn cleaves the pro-forms of interleukin-1 beta (IL-1β) and IL-18 to bioactive forms[4].

Different subsets of inflammasomes are activated by different stimuli. NLRC4 inflammasome is activated by flagellin and the type III secretion apparatus from bacteria[5-7]. Anthrax lethal toxin produced by *Bacillus anthracis* triggers activation of NLRP1B inflammasome in murine macrophages[8]. NLRP3 inflammasome activation depends on a priming step (signal 1) and an activation step (signal 2)[9]. Signal 1 can be induced by toll-like receptor (TLR) signaling, while signal 2 is induced by microbial components with diverse molecular structures, such as microbial RNA and toxins[10,11]. In addition, the adjuvant alum and endogenous danger-associated molecules, including ATP and monosodium urate (MSU) crystals, also induce signal 2 for the activation of the NLRP3 inflammasome[10,12,13]. AIM2 and IFI16 sense cytosolic and nuclear DNA, respectively, and DNA viruses[14], *Francisella tularensis*[15], *Listeria monocytogenes*[16,17], and *Streptococcus pneumoniae*[18] have been demonstrated to activate the AIM2 or IFI16[19] inflammasome in host cells.

The adaptor molecule ASC (also known as PYCARD, TMS-1) is composed of a pyrin domain and a CARD domain and contributes to the assembly of inflammasome complexes[20]. ASC serves as the bridge between pro-caspase-1 and pyrin-containing inflammasome members, such as NLRP3 and AIM2. Accordingly, NLRP3 and AIM2 require ASC exclusively for recruiting pro-caspase-1, while CARD-containing receptors, NLRC4 and NLRP1, can directly interact with pro-caspase-1[1,7,21]. During inflammasome activation, ASC also forms cytosolic macromolecular aggregates of ASC dimers termed ASC specks, ASC foci, or pyroptosomes[22,23]. The ASC speck recruits and activates pro-caspase-1, leading to the secretion of robust amounts of IL-1β and IL-18 and to pyroptosis, a form of programmed cell death. ASC is, however, not always essential for cytokine processing and pyroptosis induction via the NLRC4 inflammasome. In addition to protein-protein interactions within inflammasome complexes, recent reports have revealed the involvement of type I IFNs[15,24], ubiquitin ligase-associated protein SGT1, heat-shock protein 90[25], unidentified serine protease(s)[26], and kinases[27-33], such as PKCδ, PKR, Syk, Lyn, PI3K, ERK and DAPK, in the activation or regulation of inflammasomes, but how these molecules participate in inflammasome activity remains largely unclear.

In the light of the significance of the protective and pathological roles for inflammasomes, it is worth clarifying what and how signaling factors are involved in the activation of inflammasomes. Here, we show that the NLRP3 and AIM2 inflammasomes, but not the NLRC4 inflammasome, require Syk and JNK for their full activity. Inhibition of Syk or JNK abolished the formation of ASC specks triggered by NLRP3 or AIM2 stimuli without affecting the interaction between ASC and the receptor. We have found that ASC undergoes Syk- and JNK-dependent phosphorylation and that Tyr144, one of the possible phosphorylation sites, is critical for speck formation. Our results have implicated the phosphorylation of ASC as a novel target for controlling inflammasome activity.

RESULTS

NLRP3 and AIM2 require Syk and JNK for IL-18 secretion

To examine the role of kinases in inflammasome activation, we tested the effects of a series of common kinase inhibitors (listed in Supplementary Table 1) on the NLRP3, AIM2 and NLRC4 inflammasomes in peritoneal macrophages. To rule out the possible effects of inhibitors on signal 1 delivered by priming with lipopolysaccharide (LPS), these inhibitors were added to macrophage cultures 3 h after the initiation of LPS priming. These inhibitors did not affect protein levels of inflammasome components, pro-IL-18, and pro-IL-1β (Supplementary Fig. 1a). IL-18 secretion was measured as an indicator of caspase-1 activation, as pro-IL-18, unlike pro-IL-1β, is constitutively expressed in macrophages[31]. IL-18 secretion from macrophages induced by nigericin was significantly diminished by pretreatment with Syk or JNK inhibitors, but not inhibitors of other kinases, compared to DMSO control (Fig. 1a). Similar results were observed when murine bone marrow-derived macrophages (BMDMs) or U937, a human macrophage cell line, were employed (Supplementary Fig. 1b,c), excluding macrophage type and species-specific effects. IL-18 production induced by alum, another NLRP3 activator, was also diminished by pretreatment with Syk or JNK inhbitor (Supplementary Fig. 1e), suggesting that Syk and JNK contribute to the activation of the NLRP3 inflammasome. Moreover, we found that IL-18 production induced by poly(dA:dT), but not by flagellin, was substantially inhibited by pretreatment with Syk or JNK inhibitors (Fig. 1b,c). To confirm the role of Syk and JNK, we used siRNA to knockdown of *Syk* and *Mapk8,Mapk9* in macrophages, or Syk- or JNK-deficient macrophages, and knockdown or knockout of either *Syk* or *Mapk8,Mapk9* decreased the secretion of IL-18 in response to nigericin or poly(dA:dT) (Fig. 1d–h and Supplementary Fig. 2a–d). Also, IL-1β secretion from macrophages induced by nigericin was reduced by Syk or JNK inhibitors or knockout of either *Syk* or *Mapk8,Mapk9* (Fig. 1e and Supplementary Fig. 1d). These observations suggested that Syk and JNK are involved in the activation of the NLRP3 and AIM2 inflammasomes. Syk deficiency in macrophages resulted in a moderate decrease in the secretion of IL-18 and IL-1β induced by nigericin, indicating that Syk is not a critical requirement for NLRP3 inflammasome activation, but rather contributes to it (Fig. 1d,e). *Salmonella* Typhimurium 14028 and *Mycobacterium tuberculosis* H37Rv are recognized mainly by NLRC4 and NLRP3, respectively, while *Listeria monocytogenes* EGD is recognized by multiple receptors, including AIM2 and NLRP3[6,17,33]. Consistent with the above ligand stimulation studies, IL-18 production induced by *S.* Typhimurium was not considerably affected by inhibition of Syk or JNK in macrophages, whereas IL-18 production induced by *M. tuberculosis* or *L. monocytogenes* was reduced by Syk or JNK inhibitors (Fig. 1i–k). From these results, we conclude that Syk and JNK contribute to the activity of the NLRP3 and AIM2 inflammasomes, but not the NLRC4 inflammasome.

Caspase-1 activation requires Syk and JNK

Next, we tested whether Syk and JNK are involved in caspase-1 activation via the NLRP3 and AIM2 inflammasomes. Activation of caspase-1 induced by nigericin, alum or poly(dA:dT) in peritoneal macrophages was almost completely abolished in the presence of Syk or JNK inhibitors but not inhibitors of other kinases (Fig. 2a,b and Supplementary Fig.

1f). In contrast, the effects of these two inhibitors were not observed on caspase-1 activation induced by flagellin or *S.* Typhimurium (Fig. 2c,d). Furthermore, caspase-1 activation induced by nigericin or poly(dA:dT) was reduced in Syk- or JNK-deficient macrophages, or by siRNA-mediated knockdown of these kinases (Fig. 2e–h and Supplementary Fig. 2e,f). Caspase-1 activation induced by *M. tuberculosis* or *L. monocytogenes* in macrophages was reduced by treatment with Syk or JNK inhibitors compared to DMSO control (data not shown). These results suggested that Syk and JNK signals are involved in caspase-1 activation through the NLRP3 and AIM2 inflammasomes but not in that depending on the NLRC4 inflammasome.

Syk is not required for NLRP3 inflammasome activation in dendritic cells

It has been reported that Syk is not required for nigericin-induced activation of the NLRP3 inflammasome in dendritic cells (DCs)[28]. Consistent with the report, no significant difference was observed between wild-type and Syk-deficient BMDCs in caspase-1 activation and IL-18 secretion in response to nigericin (Supplementary Fig. 3a,c,d). By contrast, IL-18 secretion and caspase-1 activation induced by nigericin were decreased in Syk-deficient peritoneal macrophages and BMDMs, as compared with control macrophages (Fig. 1d,e, 2e and Supplementary Fig. 3b,e). This suggests that Syk requirement for NLRP3 activation in response to nigericin is cell type-specific.

Syk and JNK regulate inflammasome activity independent of ROS and CARD9

We tested whether inflammasome-activating agents induce the activation of Syk and JNK as determined by detection of phosphorylated kinases. Stimulation with nigericin or poly(dA:dT) induced detectable levels of phospho-Syk and phospho-JNK (Supplementary Fig. 4a–d). JNK phosphorylation induced by nigericin or poly(dA:dT) was not reduced by Syk inhibitors or in Syk-deficient peritoneal macrophages (Supplementary Fig. 4e–g), suggesting that Syk is not upstream of JNK. Syk has been reported to play a pivotal role in the activation of the NLRP3 inflammasome in response to *Candida albicans* by inducing the generation of reactive oxygen species (ROS) and CARD9-dependent activation of NF-κB[28]. However, we observed that wild-type and CARD9-deficient macrophages produced comparable levels of IL-18 in response to nigericin or poly(dA:dT) and that the ROS scavenger butylated hydroxyanisole (BHA) did not affect the activation of the AIM2 inflammasome in macrophages (Supplementary Fig. 4h–j). Moreover, expression of mitochondrial ROS, which is important for the activation of NLRP3, was not reduced by Syk or JNK inhibitors in nigericin-stimulated macrophages (Supplementary Fig. 4k). These results indicated that Syk- and JNK-dependent activation of the inflammasome is not mediated by ROS or CARD9, and implying that Syk and JNK operate in a different pathway(s).

Syk and JNK are required for the formation of ASC specks

Both NLRP3 and AIM2 require the common adaptor ASC to recruit and activate pro-caspase-1[1]. We therefore speculated that Syk and JNK might be involved in the interaction of ASC with the receptors. To test this possibility, ASC-NLRP3 complexes were visualized by an *in situ* Proximity Ligation Assay (PLA). As reported[30], small spots of ASC-NLRP3 complexes were observed and increased upon stimulation with nigericin in peritoneal

macrophages (Fig. 3a). The spots were not increased by nigericin stimulation in the absence of ASC or NLRP3 (data not shown), suggesting that ASC-NLRP3 complexes were specifically visualized by this technique. The number of spots representing ASC-NLRP3 complexes was similar in macrophages pretreated with Syk or JNK inhibitors and untreated macrophages upon stimulation with nigericin (Fig. 3a,b), indicating that Syk and JNK inhibition did not affect the interaction between NLRP3 and ASC, a critical step in NLRP3 inflammasome formation, in macrophages stimulated with nigericin. Next, we visualized ASC speck formation and found that pretreatment with Syk or JNK inhibitors or either Syk or JNK deficiency reduced the formation of ASC specks induced by nigericin in macrophages (Fig. 3c–f and Supplementary Fig. 5a,b). Because ASC has been reported to form Triton X-100-resistant aggregates[20], Triton X-100-soluble and -insoluble fractions from macrophages were prepared to analyze the distribution of ASC. ASC was hardly detected in the Triton X-100-insoluble fraction of LPS-primed macrophages, but was significantly increased after stimulation with nigericin (Fig. 3g). Moreover, the majority of ASC in the Triton X-100-insoluble fraction was dimerized or oligomerized[15] (Fig. 3h). Pretreatment with Syk or JNK inhibitors reduced the redistribution of ASC induced by nigericin, also resulting in a decrease in the amount of dimerized and oligomerized ASC (Fig. 3g,h). Similar results were obtained in macrophages stimulated with poly(dA:dT) (Fig. 3i,j and Supplementary Fig. 5c–f). These results suggested that Syk and JNK signals are required for the formation of ASC specks but not NLR-ASC interaction.

ASC is phosphorylated upon inflammasome activation in macrophages

A previous report has implied that ASC undergoes phosphorylation in response to inflammatory stimuli[34]. To test whether aggregate formation of ASC was regulated by its phosphorylation mediated by Syk and JNK during inflammasome activation, phosphorylated proteins were enriched from macrophage lysates using a column containing a phosphoprotein-binding resin and analyzed for the presence of ASC by immunoblotting. We observed that nigericin stimulation induced an increase in the amount of ASC in the elution fraction (enriched phosphoproteins; Fig. 4a). To further analyze the phosphorylation of ASC, the Triton X-100-soluble and -insoluble cell lysates were subjected to the Phos-tag-based mobility shift assay (Phos-tag MSA)[35]. In Phos-tag gels, ASC in the Triton X-100-insoluble fraction migrated more slowly than that in the Triton X-100-soluble fraction, and the mobility shift was reversed by phosphatase treatment, suggesting that ASC in the former fraction is phosphorylated (Fig. 4b,c). The slow-migrating ASC was observed in the Triton X-100-insoluble fraction of caspase-1-deficient macrophages, but not in that of NLRP3-deficient macrophages, after nigericin stimulation, suggesting that the increase in phosphorylated ASC in response to nigericin requires NLRP3 but not caspase-1 (Fig. 4b). ASC may be phosphorylated at multiple sites, as three major bands with different mobility were detected (closed triangles in Fig. 4c–g). In addition, deficiency of either Syk or JNK decreased the intensity of the ASC band with the lowest mobility in the Triton X-100-insoluble fraction of macrophages stimulated with nigericin or poly(dA:dT) (Fig. 4d–g). Similar results were obtained when Syk or JNK were inhibited with Syk or JNK inhibitors, respectively (data not shown). These data suggested that ASC is phosphorylated upon the activation of the NLRP3 and AIM2 inflammasomes via the Syk and JNK pathways. Syk and DAPK have been shown to associate with the NLRP3 inflammasome complex[29,30].

Accordingly, we analyzed the interaction of ASC with phospho-JNK by the *in situ* PLA. ASC-phospho-JNK complexes were observed in wild-type macrophages (Fig. 4h–k), but not in ASC-deficient macrophages (negative control; data not shown), upon stimulation with nigericin or poly(dA:dT). Notably, most of the complexes were located in or around the nucleus at later time points (Fig. 4h,j). These data suggested that ASC is phosphorylated upon the activation of the NLRP3 and AIM2 inflammasomes via the Syk and JNK pathways.

Phosphorylation of ASC is critical for inflammasome activation

We next tried to identify the ASC phosphorylation sites that may regulate the aggregate formation resulting in caspase-1 activation. The total of 14 or 8 possible phosphorylation sites were detected in murine ASC by NetPhos 2.0 at a threshold of 0.5 or Group-based Prediction System 2.1.1 with the low threshold, respectively (Supplementary Fig. 6 and Supplementary Table 2). A series of expression vectors encoding ASC mutants were constructed, in which amino acid residues predicted to be phosphorylated were replaced by alanine or phenylalanine residues, and the point mutants of ASC were tested for their ability to induce IL-1β secretion in an HEK293 cell-based inflammasome reconstitution system (Supplementary Fig. 7a,b). We observed that the ability of ASC (S58A), ASC (T125A), ASC (Y144F), and ASC (T151A,T152A,S153A) to induce IL-1β secretion in response to NLRP3 (R258W), a disease-associated NLRP3 mutant, was partially reduced compared to that of wild-type ASC (Fig. 5a,b). The ASC (S58A) variant was further mutated at Thr125 (58–125) or Thr151,Thr152,Ser153 (58–151), and IL-1β-inducing ability of the resulting ASC variants was significantly lower than that of ASC (S58A) (Fig. 5b). Furthermore, ASC (Y144F) and ASC (58–151) showed less redistribution into the Triton X-100-insoluble fraction in response to NLRP3 (R258W) (Fig. 5c,d). ASC (Y144F) and ASC (58–151) were still capable of forming dimers and oligomers in the Triton X-100-insoluble fraction (Fig. 5e), likely because these mutations affected the redistribution of ASC without affecting their dimerization or oligomerization. Moreover, we found that ASC (Y144F) co-expressed with NLRP3 (R258W) hardly formed aggregates, in contrast with HEK293 cells transfected with wild-type ASC together with NLRP3 (R258W) (Fig. 5f). These results suggested that Tyr144, Ser58, Thr151, Thr152 and Ser153, which are putative phosphorylation sites of ASC, are involved in both IL-1β-inducing ability and aggregate formation.

We tested whether these observations in HEK293 cell could be reproduced in a murine macrophage cell line, RAW264.7, which lacks ASC expression. Wild-type ASC co-expressed with NLRP3 (R258W) formed speck-like structures and induced the activation of caspase-1, whereas speck formation was diminished in RAW264.7 cells transfected with ASC (Y144F) or ASC (58–151) (Fig. 6a–c). ASC speck formation was also abrogated by the mutations in similar experiments using ASC-deficient primary macrophages (Fig. 6d).

We further investigated whether these residues are phosphorylated in a Syk- and JNK-dependent manner. ASC co-expressed with either Syk or JNK migrated more slowly in Phos-tag gels compared with that co-transfected with empty vector (Fig. 7a). Co-transfection of ASC with both Syk and JNK resulted in a greater mobility shift, which was reversed by phosphatase treatment (Fig. 7a,b). These results suggested that ASC is phosphorylated at

multiple sites in a Syk and JNK-dependent manner. The observed mobility changes of ASC in the presence of Syk or JNK were all abrogated by the Y144F mutation (Fig. 7c). On the other hand, the mobility of ASC (S58A), ASC (T151A,T152A,S153A) and ASC (58–151) in Phos-tag gels, like that of wild-type ASC, was reduced by overexpression of JNK1/2, suggesting that Ser58, Thr151, Thr152 and Ser153 are not phosphorylated in a JNK-dependent manner or that the effect of these mutations on the mobility may be masked by phosphorylation at other residues (Fig. 7d). These results show that Tyr144 phosphorylation is required for inflammasome activation.

We carried out *in vitro* kinase assays using synthetic peptides, mouse $ASC_{139\text{-}150}$ and human $ASC_{141\text{-}152}$, to test the possibility that Syk directly phosphorylates Tyr144 of mouse ASC and the corresponding tyrosine residue of human ASC. The peptides were incubated with ATP in the presence or absence of recombinant Syk, and kinase reaction was determined as indicated by the consumption of ATP. No significant reduction of ATP was observed in reactions in which $mASC_{139\text{-}150}$ or $hASC_{141\text{-}152}$ was used as a substrate for rSyk, whereas ATP was reduced in those containing purified tubulin, a positive control substrate (data not show). Thus, our present data do not support or are not sufficient to justify direct phosphorylation of Tyr144 by Syk.

MSU and alum-induced peritonitis is dependent on Syk and JNK

Next we tested whether Syk and JNK are required for inflammasome activation *in vivo*. Recruitment of inflammatory cells into the peritoneal cavity was analyzed as an indicator of stimulant-induced inflammation following MSU and alum intraperitoneally injection into mice. As shown previously[12,29], both MSU and alum strongly induced the recruitment of cells, including Gr-1^+ F4/80^- neutrophils and F4/80^+ monocytes and macrophages, in an ASC-dependent manner (Supplementary Fig. 8a–f). The numbers of total cells, neutrophils, and monocytes and macrophages in the peritoneal cavity upon MSU or alum challenge were decreased in *Syk*$^{-/-}$ chimeric mice compared to *Syk*$^{+/-}$ chimeric mice (Fig. 8a,b,d–f). The number of peritoneal monocytes and macrophages upon MSU challenge tended to be lower in *Syk*$^{-/-}$ chimeric mice than in *Syk*$^{+/-}$ chimeric mice, but there was no statistical difference between the groups (Fig. 8c). The infiltration of inflammatory cells induced by MSU or alum was also decreased in *Mapk8*$^{-/-}$ chimeric mice or in mice treated with JNK inhibitor compared to *Mapk8*$^{+/+}$ chimeric mice or mice that received vehicle only, respectively (Fig. 8g–i and Supplementary Fig. 8a–f). By contrast, inflammasome-independent infiltration of inflammatory cells induced by KC was comparable in *Syk*$^{+/-}$ and *Syk*$^{-/-}$ chimeric mice and in *Mapk8*$^{+/+}$ and *Mapk8*$^{-/-}$ chimeric mice (Supplementary Fig. 8g–l), and JNK inhibitor did not reduce inflammatory cell infiltration induced by alum in ASC-deficient mice (n = 3, data not shown). These results suggested that Syk and JNK signals are involved in the MSU- and alum-induced infiltration of inflammatory cells that is largely dependent on ASC.

DISCUSSION

Protein phosphorylation and dephosphorylation is important in controlling a wide range of biological processes including innate and adaptive immunity and apoptosis[36,37]. Recently the involvement of kinases, such as PKCδ, PKR, Syk, Lyn, PI3K, ERK and DAPK was

reported in inflammasome activation, yet the precise mechanism of their action is not clear. In particular, Syk has been demonstrated to contribute to the NLRP3 inflammasome in response to *Candida albicans*, most likely due to its role in inducing ROS production[28,29,31,33]. NLRC4 was shown to be phosphorylated following ligand stimulation and that the phosphorylation is critical for inflammasome activation[27]. In the present study, we show that Syk and JNK are involved in the activity of ASC-containing inflammasomes in macrophages via a mechanism that regulates formation of ASC specks. We found that ASC can be phosphorylated in a Syk- and JNK-dependent manner at multiple sites, which most likely include Tyr144 essentially required for speck formation. ASC phosphorylation during inflammasome activation is required for the activity of the NLRP3 and AIM2 inflammasomes. Thus, inflammasomes are regulated by protein kinases, and perhaps by phosphatase(s) targeting phosphorylated inflammasome components.

We identified Tyr144 of ASC as a critical residue for speck formation and a possible phosphorylation site. Consistently, phosphorylation of the corresponding residue in human ASC, Tyr146, has been disclosed in US patent application (Hornbeck et al. Pub. No.: US 2009/0325189 A1). The Y144F mutation completely abrogated the phosphorylation of ASC induced by overexpression of Syk or JNK, suggesting that Tyr144 serves as a regulator of ASC phosphorylation mediated by these kinases. This tyrosine residue is evolutionary conserved. Tyr144 is located in the CARD domain, while previous studies have shown that the pyrin domain of ASC is phosphorylated following stimulation with tumor necrosis factor[34], suggesting the existence of other phosphorylation sites which may also contribute to inflammasome activity.

It remains unclear how Syk and JNK signals regulate ASC speck formation. Transfection of HEK293 cells with ASC together with Syk, JNK or both did not result in the formation of ASC specks and the redistribution of ASC to the Triton X-100-insoluble fraction (data not shown), suggesting that phosphorylation of ASC itself is not sufficient to induce speck formation in the absence of inflammasome stimuli. Our results also suggested that Syk and JNK play a crucial role in redistribution, rather than dimerization and oligomerization, of ASC upon inflammasome activation. During the generation of ASC aggregates, monomeric ASC, which is diffusely distributed before stimulation, is rapidly translocated to a perinuclear speck in each cell. It has been demonstrated that ASC speck formation is prevented by nocodazole treatment and that ASC specks are localized near the microtubule-organizing center[38], suggesting a possible role of microtubules in the migration of ASC during the step of speck formation. In our assays the majority of ASC-phospho-JNK complexes were located in or around the nucleus and ASC remained diffusely in the cytosol even after inflammasome activation if Syk or JNK was inhibited genetically or pharmacologically. Thus, we speculate that Syk and JNK-mediated ASC phosphorylation may function as a molecular switch controlling the migration of ASC along microtubules to the site of speck formation. Taken together, ASC speck formation is a consequence of multiple cellular events orchestrated by inflammasome receptors, Syk, JNK and perhaps microtubules.

Although inflammasomes play pivotal roles in innate immunity against pathogens, excessive or dysregulated activation of inflammasomes, especially the NLRP3 inflammasome, is

implicated in a number of auto-inflammatory diseases and autoimmune diseases, including Muckle-Wells syndrome, inflammatory bowel diseases[39,40], vitiligo[41] and rheumatoid arthritis[12]. The inflammasome has also been implicated in obesity-induced insulin resistance[42], atherosclerosis[43] and gouty arthritis[44] and could represent potential targets for therapy. Anti-IL-1β therapies appear to be effective in treating inflammatory disorders associated with deregulated inflammasome activity, and further understanding of basic processes and mechanisms involved in inflammasome activation will provide novel strategies for controlling auto-inflammatory conditions. In the present study, we have shown that phosphorylation of the inflammasome component ASC regulates inflammasome activity. Thus, for example, compounds designated to specifically inhibit ASC phosphorylation may be promising drug candidates for treating inflammasome-associated diseases and antibodies specific to phosphorylated ASC may be useful for diagnostic and research purposes. Further investigations of the inflammasome will reveal the precise roles of kinases in inflammasome activation and may identify additional mechanisms controlling inflammasome activity.

METHODS

Mice

Wild-type, *Casp1*$^{-/-}$, *Pycard*$^{-/-}$, *NLRP3*$^{-/-}$, *CARD9*$^{-/-}$, *Mapk8*$^{-/-}$ and *Mapk9*$^{-/-}$ female C57BL/6J mice were maintained in specific-pathogen-free conditions and used at 6–9 weeks of age[12,16,45,46]. C57BL/6J mice heterozygous for the *Syk*^{tm1Tyb} allele[47] were intercrossed to generate embryos at embryonic day 16.5 that were wild-type for the *Syk* gene (*Syk*$^{+/+}$) or heterozygous or homozygous for the *Syk*^{tm1Tyb} allele (*Syk*$^{+/-}$ or *Syk*$^{-/-}$). Fetal liver cells from these embryos were used to reconstitute C57BL/6J mice that had been irradiated with a total dose of 10 Gy from a ^{137}Cs source. Bone marrow cells from wild-type, *Mapk8*$^{-/-}$, or *Mapk9*$^{-/-}$ mice were also used to reconstitute irradiated C57BL/6J mice. Mice were used 6–7 weeks after reconstitution. All the experimental procedures performed on mice were approved by the Animal Ethics and Research Committee of Kyoto University Graduate School of Medicine.

Cells

Peritoneal macrophages, BMDMs and BMDCs were prepared as reported[48,49]. These cells suspended in culture medium consisted of RPMI 1640 supplemented with 10% FCS and 10 μg/ml gentamicin were incubated on culture plates at 37°C for overnight, then used for this study. U937 cells provided by Dr. Matsuura were cultured in culture medium supplemented with 10 ng/ml of 12-*O*-tetradecanoylphorbol 13-acetate, 100 U/ml of penicillin and 100 μg/ml of streptomycin for 3 days. The order of treatment and positions of wells within multi-well devices were determined in a random fashion.

Reagents

LPS and flagellin were purchased from Invivogen, alum from Pierce, nigericin and poly(dA:dT) from Sigma-Aldrich, MSU from Nacalai tesque, R406 from Selleckchem, other kinase inhibitors from Merck Biosciences, and BHA from Wako. Anti-ASC polyclonal antibody (AL177) and anti-NLRP3 mouse monoclonal antibody (mAb) (Cryo-2) were

purchased from Alexis, anti-JNK mAb (56G8), anti-phospho-JNK mAb (81E11) and anti-phospho-JNK mouse mAb (G9) from Cell Signaling Technology, anti-phospho-Tyr mAb (PY20), anti-caspase-1 p10 antibody, and anti-Syk antibody from Santa Cruz, anti-FLAG antibody from Rockland Immunochemicals, biotin-conjugated anti-IL-1β antibody from R&D Systems, and anti-IL-18 mAb (39-3F) from MBL. The ELISA kit for mouse IL-1β was purchased from eBioscience. For the titration of human or mouse IL-18, a pair of biotin-labeled and -unlabeled monoclonal antibodies specific to IL-18 (MBL) was used.

Plasmids

The pmax-GFP plasmid was purchased from Lonza. The pFLAG expression vectors for ASC, pro-caspase-1, and pro-IL-1β were previously constructed[16]. The expression vectors for NLRP3 (R258W), Syk, JNK1 (isoform β2), and JNK2 (isoform β2) were constructed by using primer sets indicated in Supplementary Table 3 and the pFLAG-CMV2 vector (Sigma-Aldrich). After the construction, the NLRP3 or ASC mutation was introduced into each expression vector by site-directed mutagenesis. Similarly, pFLAG-pro-caspase-1 and pFLAG-pro-IL-1β, in which the FLAG-tag was removed, were generated.

Stimulation with inflammasome activators

Cells were plated at 5×10^5 cells/well in 24-well microplates. Culture medium was replaced with Opti-MEM (Invitrogen) prior to stimulation or infection. Macrophages were primed with 50 ng/ml LPS for 4 h, and stimulated with nigericin (5 μM) or alum (500 μg/ml). To deliver into the cytosol of macrophages, flagellin (15 ng) was encapsulated into Sendai virus envelope using GenomONE-Neo (Ishihara Sangyo). Poly(dA:dT) (2.6 μg/ml) was introduced into unprimed macrophages using Lipofectamine LTX (Invitrogen). Cells were infected with *L. monocytogenes* EGD[48] (MOI = 1) or *S.* Typhimurium 14028 (MOI = 10), and gentamicin was added to the cultures 30 min after infection. Cells infected with *M. tuberculosis* H37Rv (MOI = 5) were washed 3 h after infection and further cultivated in Opti-MEM containing gentamicin. Kinase inhibitors or dimethyl sulfoxide (DMSO) were added to cell cultures 1 h before stimulation or infection for inflammasome activation.

Immunoblotting

Cells were lysed with SDS sample buffer. Supernatants were concentrated using trichloroacetate. To generate the Triton X-100-soluble and -insoluble fractions, cells were lysed with 50 mM Tris-HCl (pH 7.6) containing 0.5% Triton X-100, EDTA-free protease inhibitor cocktail and phosphatase inhibitor cocktail (Nacalai tesque). The lysates were centrifuged at 6,000*g* at 4 °C for 15 min, and the pellets and supernatants were used as the Triton-insoluble and -soluble fractions, respectively. To detect phospho-Syk, total Syk was immunoprecipitated with anti-Syk antibody and protein G-sepharose (GE Healthcare).

Cross-link of ASC dimers or oligomers

The Triton-insoluble pellets were washed with Tris-buffered saline (TBS) two times and then resuspended in 500 μl of TBS. The resuspended pellets were cross-linked with 2 mM disuccinimidyl suberate (DSS; Pierce) for 45 min at 37 °C, and then centrifuged at 6,000*g* for 15 min. The pellets were dissolved in SDS sample buffer.

Enrichment of phosphoproteins

Phosphoproteins were enriched from cell lysates by using Pro-Q Diamond phosphoprotein enrichment Kit (Invitrogen), according to the manufacturer's instructions. Cells were lysed in lysis buffer supplemented with endonuclease and proteinase inhibitors, then ASC aggregates were solubilized with 8 M urea. After centrifugation at 10,000 *g* for 10 min, the supernatants were applied to the Pro-Q diamond column (1 mg protein/column). The column was washed and eluted with elution buffer (50 mM Tris, 2% SDS, 10 mM EDTA, 5% 2-mercaptoethanol, pH 8). The flow-through and elution fractions were concentrated using trichloroacetate. ASC or phospho-Tyr in each fraction was detected by immunoblotting.

Phos-tag-based Mobility Shift Assay

The Triton X-100-insoluble and -soluble fractions from macrophages prepared as described above were subjected to the Phos-tag MSA. HEK293 cells were lysed with 50 mM Tris-HCl (pH 7.6) containing 1% SDS, precipitated with isopropanol and acetone. Proteins in the cell lysates were precipitated with acetone, incubated in phosphatase reaction mixture containing 250 U/ml of antarctic phosphatase (New England Biolabs) overnight at 37°C, reprecipitated with acetone and dissolved in SDS sample buffer. These samples were electrophoresed in 12% polyacrylamide gels with or without 50 μM $MnCl_2$ and 25 μM Phos-tag ligand (NARD Institute).

RNA interference

Cells were transfected with 30 nM small interfering RNAs (siRNAs) using siPORT Amine Transfection Agent (Ambion) as reported[16]. After 48 h cultivation, the cells were washed and used in experiments. Sense siRNA sequences were; *Syk* (A), ACU UGU AGU AGU UGA UGC AUU CGG G; *Syk* (B), AUU CCG AUC AUG CGC ACA AUG UAG G; *Mapk8* (A), AAU AUA GUC CCU UCC UGG AAA GAG G; *Mapk8* (B), AAU UCC AGC AGA GUG AAG GUG CUU G; *Mapk9* (A), UAA AGU UGG UAC AGG CUG UUC GCG C; *Mapk9* (B), UUC AAU CGC AUG CUC UCU UUC UUC C. Stealth RNAi negative control medium GC duplex #3 was purchased from Invitrogen.

Immunofluorescence staining

Cells seeded in 8-well chamber plates at 2.5×10^5 cells/well were washed two times, fixed in 4% paraformaldehyde and permeabilized with 0.25% Triton X-100. The cells were incubated with anti-ASC antibody and then with Alexa 488-labeled or Alexa 594-labeled anti-rabbit IgG antibody (Invitrogen). Nuclei were stained with DAPI (Dojindo).

In situ Proximity Ligation Assay

Fixed and permeabilized cells were incubated with pairs of primary antibodies, rabbit anti-ASC antibody together with mouse anti-phospho-JNK mAb or mouse anti-NLRP3 mAb overnight at 4 °C. The cells were washed and reacted with a pair of proximity probes (Olink Bioscience). The rest of the *in situ* PLA protocol was performed according to the manufacturer's instructions. The cells were examined under a fluorescent microscope (Olympus), and quantitative analysis was performed by using Duolink Image Tool (Olink Bioscience).

Reconstruction of the inflammasome system in HEK293 cells

HEK293 cells (CRL-1573) obtained from the American Type Culture Collection were maintained in DMEM supplemented with 10% FCS, 6 mM L-glutamine, 1 mM sodium pyruvate and 5 μg/ml gentamicin as described[16]. For experiments, HEK293 cells were plated in 24-well microplates at a density of 2×10^5 cells/well and incubated overnight. The cells were transfected with plasmids using Transfectin (Bio-Rad) according to the manufacturer's instructions. The total amount of DNA was adjusted to 1 μg/well with pFLAG-CMV2 empty vector. The cells were washed with culture medium 36 h after transfection and further incubated for 12 h.

Reconstruction in macrophages

RAW264.7 cells provided by Dr. Tanizaki or primary *Pycard*$^{-/-}$ peritoneal macrophages were transfected with 1000 ng of pFLAG-ASC or the ASC mutant vectors together with pFLAG-NLRP3 (R258W) (250 ng) using Neon Transfection System (Invitrogen) according to the manufacturer's instructions. Electroporation parameters were as indicated below; Pulse voltage 1,680 V; Pulse width 20 ms, Pulse number 1, Cell number 1×10^6 cells. The cells were incubated for 9 h.

Peritonitis

Mice were intraperitoneally challenged with MSU (1 mg) or alum (0.4 mg). Two hours before and 30 min after challenge with the irritants, wild-type mice were intraperitoneally treated with DMSO or JNK inhibitor SP600125 (25 mg/kg). The mice were sacrificed 6 h after injection of the stimuli, and peritoneal cavities were lavaged with 5 ml of PBS. Mice were intraperitoneally injected with mouse KC (CXCL1; 0.8 μg, BioLegend) or PBS and peritoneal cells were collected 1.5 h after stimulation. Peritoneal cells were counted by using Countess (Invitrogen) and then reacted with anti-mouse CD16 mAb (BioLegend). The cells were subsequently stained with FITC-labeled anti-Gr-1 mAb (RB6-8C5, BioLegend) and PE-labeled anti-F4/80 mAb (BM8, BioLegend) and analyzed on a FACSCalibur (Becton-Dickinson). Mice were prepared by H.H. and randomly assigned to experimental groups. Another investigator R.F., who performed injection and flow cytometric analyses, was blinded to the groups.

Statistical analysis

Sample size of *in vivo* and *in vitro* studies was chosen as small as possible but allowing the evaluation of distribution normality. For two-group comparisons with Gaussian distribution, the two-tailed unpaired *t*-test with Welch's correction was used when the variances of the groups were judged to be equal by the *F* test. For two-group comparisons with non-Gaussian distribution, Mann-Whitney test was used. Multi-group comparisons with Gaussian distribution, one-way analysis of variance (ANOVA) with Bonferroni or Tukey-Kramer (in the case of unequal sample size) multiple comparison test was used after the confirmation of homogeneity of variance among the groups using Bartlett's test. Multi-group comparisons with non-Gaussian distribution, Kruskal-Wallis test with Dunn's test was used. *P* values of 0.05 or less were the threshold for statistical significance.

Supplementary Material

Refer to Web version on PubMed Central for supplementary material.

ACKNOWLEDGMENTS

We thank J. Tschopp (University of Lausanne) and the Institute for Arthritis Research for permission to use *NLRP3*$^{-/-}$ mice; S.Taniguchi (Shinshu University) for *Pycard*$^{-/-}$ mice; K. Kuida (Millennium Pharmaceuticals) for *Casp1*$^{-/-}$ mice; T. Saito (RIKEN RCAI) for *CARD9*$^{-/-}$ mice; K. Kawasaki (Doshisha Women's College) for *Salmonella* Typhimurium 14028 strain; K. Sada (University of Fukui) and Y. Tohyama (Himeji Dokkyo University) for providing advice on Syk experiments. We also thank H. Tsutsui (Hyogo Medical University) for providing *NLRP3*$^{-/-}$, *Pycard*$^{-/-}$ and *Casp1*$^{-/-}$ mice; H. Hara (Saga University) for *CARD9*$^{-/-}$ mice; M. Matsuura (Kyoto University) for *Salmonella* Typhimurium 14028 strain and U937 cells; H. Tanizaki (Kyoto University) for RAW264.7 cells. This work was supported by Grants-in-Aid from the Ministry of Education, Culture, Sports, Science and Technology of Japan, the Ministry of Health, Labour and Welfare of Japan, and the Japan Society for the Promotion of Science. ES and VT were supported by the Medical Research Council UK (program number U117527252).

REFERENCES

1. Martinon F, Mayor A, Tschopp J. The inflammasomes: guardians of the body. Annu. Rev. Immunol. 2009; 27:229–265. [PubMed: 19302040]
2. Brodsky IE, Monack D. NLR-mediated control of inflammasome assembly in the host response against bacterial pathogens. Semin. Immunol. 2009; 21:199–207. [PubMed: 19539499]
3. Davis BK, Wen H, Ting JP. The inflammasome NLRs in immunity, inflammation, and associated diseases. Annu. Rev. Immunol. 2011; 29:707–735. [PubMed: 21219188]
4. Dinarello CA. Immunological and inflammatory functions of the interleukin-1 family. Annu. Rev. Immunol. 2009; 27:519–550. [PubMed: 19302047]
5. Miao EA, et al. Innate immune detection of the type III secretion apparatus through the NLRC4 inflammasome. Proc. Natl. Acad. Sci. U S A. 2010; 107:3076–3080. [PubMed: 20133635]
6. Franchi L, et al. Cytosolic flagellin requires Ipaf for activation of caspase-1 and interleukin 1beta in salmonella-infected macrophages. Nat. Immunol. 2006; 7:576–582. [PubMed: 16648852]
7. Miao EA, et al. Cytoplasmic flagellin activates caspase-1 and secretion of interleukin 1beta via Ipaf. Nat. Immunol. 2006; 7:569–575. [PubMed: 16648853]
8. Boyden ED, Dietrich WF. Nalp1b controls mouse macrophage susceptibility to anthrax lethal toxin. Nat. Genet. 2006; 38:240–244. [PubMed: 16429160]
9. Franchi L, Munoz-Planillo R, Reimer T, Eigenbrod T, Nunez G. Inflammasomes as microbial sensors. Eur. J. Immunol. 2010; 40:611–615. [PubMed: 20201013]
10. Mariathasan S, et al. Cryopyrin activates the inflammasome in response to toxins and ATP. Nature. 2006; 440:228–232. [PubMed: 16407890]
11. Kanneganti TD, et al. Critical role for Cryopyrin/Nalp3 in activation of caspase-1 in response to viral infection and double-stranded RNA. J. Biol. Chem. 2006; 281:36560–36568. [PubMed: 17008311]
12. Martinon F, Petrilli V, Mayor A, Tardivel A, Tschopp J. Gout-associated uric acid crystals activate the NALP3 inflammasome. Nature. 2006; 440:237–241. [PubMed: 16407889]
13. Li H, Nookala S, Re F. Aluminum hydroxide adjuvants activate caspase-1 and induce IL-1beta and IL-18 release. J. Immunol. 2007; 178:5271–5276. [PubMed: 17404311]
14. Rathinam VA, et al. The AIM2 inflammasome is essential for host defense against cytosolic bacteria and DNA viruses. Nat. Immunol. 2010; 11:395–402. [PubMed: 20351692]
15. Fernandes-Alnemri T, et al. The AIM2 inflammasome is critical for innate immunity to Francisella tularensis. Nat. Immunol. 2010; 11:385–393. [PubMed: 20351693]
16. Tsuchiya K, et al. Involvement of absent in melanoma 2 in inflammasome activation in macrophages infected with *Listeria monocytogenes*. J. Immunol. 2010; 185:1186–1195. [PubMed: 20566831]

17. Kim S, et al. *Listeria monocytogenes* is sensed by the NLRP3 and AIM2 inflammasome. Eur. J. Immunol. 2010; 40:1545–1551. [PubMed: 20333626]
18. Fang R, et al. Critical roles of ASC inflammasomes in caspase-1 activation and host innate resistance to *Streptococcus pneumoniae* infection. J. Immunol. 2011; 187:4890–4899. [PubMed: 21957143]
19. Kerur N, et al. IFI16 acts as a nuclear pathogen sensor to induce the inflammasome in response to Kaposi Sarcoma-associated herpesvirus infection. Cell Host Microbe. 2011; 9:363–375. [PubMed: 21575908]
20. Masumoto J, et al. ASC, a novel 22-kDa protein, aggregates during apoptosis of human promyelocytic leukemia HL-60 cells. J. Biol. Chem. 1999; 274:33835–33838. [PubMed: 10567338]
21. Case CL, Shin S, Roy CR. Asc and Ipaf Inflammasomes direct distinct pathways for caspase-1 activation in response to *Legionella pneumophila*. Infect. Immun. 2009; 77:1981–1991. [PubMed: 19237518]
22. Bryan NB, Dorfleutner A, Rojanasakul Y, Stehlik C. Activation of inflammasomes requires intracellular redistribution of the apoptotic speck-like protein containing a caspase recruitment domain. J. Immunol. 2009; 182:3173–3182. [PubMed: 19234215]
23. Fernandes-Alnemri T, et al. The pyroptosome: a supramolecular assembly of ASC dimers mediating inflammatory cell death via caspase-1 activation. Cell Death Differ. 2007; 14:1590–1604. [PubMed: 17599095]
24. Guarda G, et al. Type I interferon inhibits interleukin-1 production and inflammasome activation. Immunity. 2011; 34:213–223. [PubMed: 21349431]
25. Mayor A, Martinon F, De Smedt T, Petrilli V, Tschopp J. A crucial function of SGT1 and HSP90 in inflammasome activity links mammalian and plant innate immune responses. Nat. Immunol. 2007; 8:497–503. [PubMed: 17435760]
26. Franchi L, et al. Calcium-independent phospholipase A2 beta is dispensable in inflammasome activation and its inhibition by bromoenol lactone. J. Innate Immun. 2009; 1:607–617. [PubMed: 20160900]
27. Qu Y, et al. Phosphorylation of NLRC4 is critical for inflammasome activation. Nature. 2012; 490:539–542. [PubMed: 22885697]
28. Gross O, et al. Syk kinase signalling couples to the Nlrp3 inflammasome for anti-fungal host defence. Nature. 2009; 459:433–436. [PubMed: 19339971]
29. Shio MT, et al. Malarial hemozoin activates the NLRP3 inflammasome through Lyn and Syk kinases. PLoS Pathog. 2009; 5:e1000559. [PubMed: 19696895]
30. Chuang YT, et al. Tumor suppressor death-associated protein kinase is required for full IL-1beta production. Blood. 2011; 117:960–970. [PubMed: 21041719]
31. Kankkunen P, et al. (1,3)-beta-glucans activate both dectin-1 and NLRP3 inflammasome in human macrophages. J. Immunol. 2010; 184:6335–6342. [PubMed: 20421639]
32. Lu B, et al. Novel role of PKR in inflammasome activation and HMGB1 release. Nature. 2012; 488:670–674. [PubMed: 22801494]
33. Wong KW, Jacobs WR Jr. Critical role for NLRP3 in necrotic death triggered by *Mycobacterium tuberculosis*. Cell. Microbiol. 2011; 13:1371–1384. [PubMed: 21740493]
34. Stehlik C, et al. The PAAD/PYRIN-only protein POP1/ASC2 is a modulator of ASC-mediated nuclear-factor-kappa B and pro-caspase-1 regulation. Biochem. J. 2003; 373:101–113. [PubMed: 12656673]
35. Kosako H, et al. Phosphoproteomics reveals new ERK MAP kinase targets and links ERK to nucleoporin-mediated nuclear transport. Nat. Struct. Mol. Biol. 2009; 16:1026–1035. [PubMed: 19767751]
36. Kurokawa M, Kornbluth S. Caspases and kinases in a death grip. Cell. 2009; 138:838–854. [PubMed: 19737514]
37. Sumbayev VV, Yasinska IM. Role of MAP kinase-dependent apoptotic pathway in innate immune responses and viral infection. Scand. J. Immunol. 2006; 63:391–400. [PubMed: 16764692]

38. Balci-Peynircioglu B, et al. Expression of ASC in renal tissues of familial mediterranean fever patients with amyloidosis: postulating a role for ASC in AA type amyloid deposition. Exp. Biol. Med. (Maywood). 2008; 233:1324–1333. [PubMed: 18791131]
39. Villani AC, et al. Common variants in the NLRP3 region contribute to Crohn's disease susceptibility. Nat. Genet. 2009; 41:71–76. [PubMed: 19098911]
40. Zaki MH, et al. The NLRP3 inflammasome protects against loss of epithelial integrity and mortality during experimental colitis. Immunity. 2010; 32:379–391. [PubMed: 20303296]
41. Jin Y, et al. NALP1 in vitiligo-associated multiple autoimmune disease. N. Engl. J. Med. 2007; 356:1216–1225. [PubMed: 17377159]
42. Vandanmagsar B, et al. The NLRP3 inflammasome instigates obesity-induced inflammation and insulin resistance. Nat. Med. 2011; 17:179–188. [PubMed: 21217695]
43. Duewell P, et al. NLRP3 inflammasomes are required for atherogenesis and activated by cholesterol crystals. Nature. 2010; 464:1357–1361. [PubMed: 20428172]
44. Pope RM, Tschopp J. The role of interleukin-1 and the inflammasome in gout: implications for therapy. Arthritis Rheum. 2007; 56:3183–3188. [PubMed: 17907163]
45. Hara H, et al. The adaptor protein CARD9 is essential for the activation of myeloid cells through ITAM-associated and Toll-like receptors. Nat. Immunol. 2007; 8:619–629. [PubMed: 17486093]
46. Cao Y, et al. Enhanced T cell-independent antibody responses in c-Jun N-terminal kinase 2 (JNK2)-deficient B cells following stimulation with CpG-1826 and anti-IgM. Immunol. Lett. 2010; 132:38–44. [PubMed: 20665951]
47. Turner M, et al. Perinatal lethality and blocked B-cell development in mice lacking the tyrosine kinase Syk. Nature. 1995; 378:298–302. [PubMed: 7477352]
48. Hara H, et al. Dependency of caspase-1 activation induced in macrophages by *Listeria monocytogenes* on cytolysin, listeriolysin O, after evasion from phagosome into the cytoplasm. J. Immunol. 2008; 180:7859–7868. [PubMed: 18523249]
49. Lutz MB, et al. An advanced culture method for generating large quantities of highly pure dendritic cells from mouse bone marrow. J. Immunol. Methods. 1999; 223:77–92. [PubMed: 10037236]

Europe PMC Funders Author Manuscripts

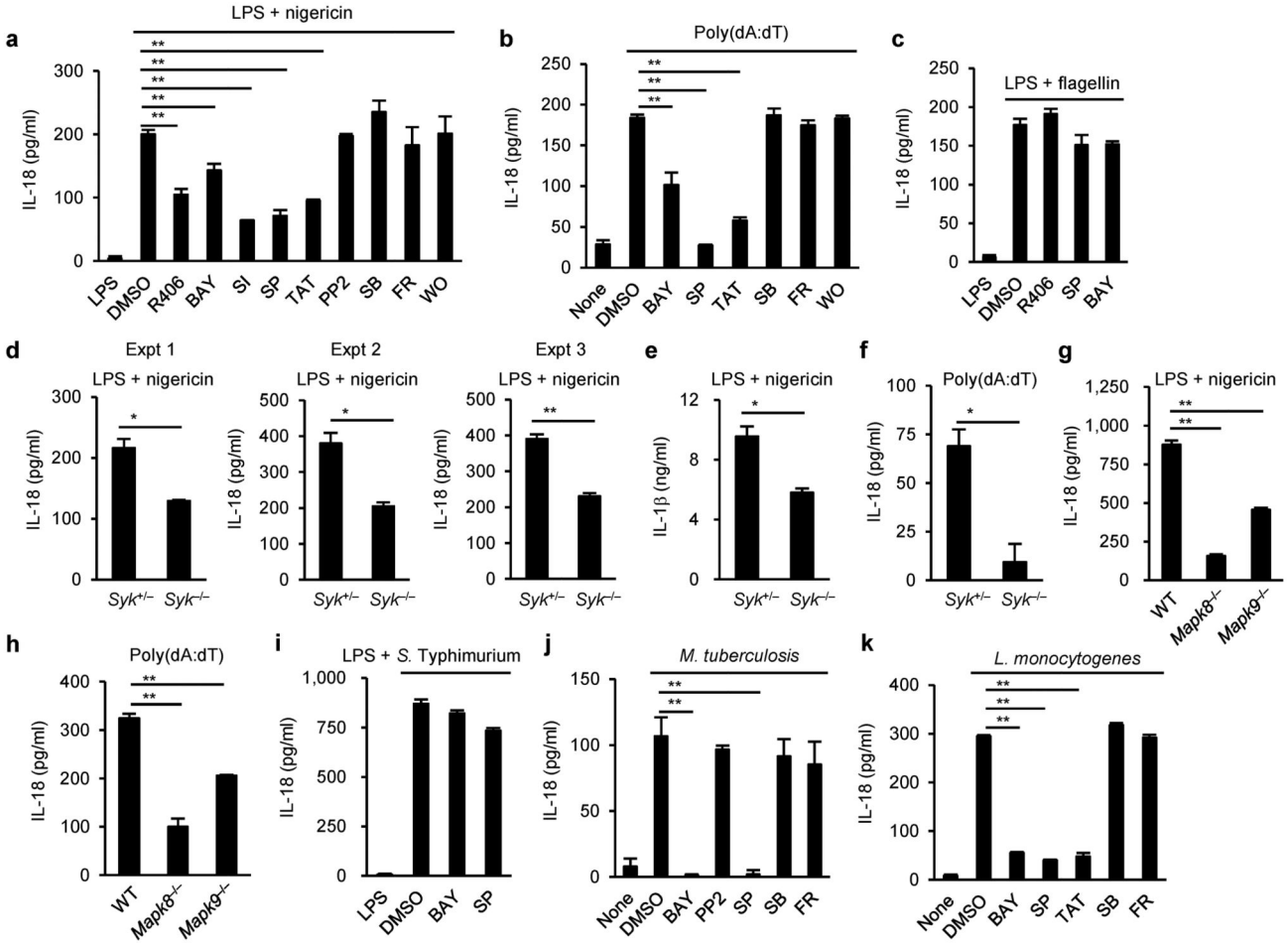

Figure 1.

Syk and JNK are required for IL-18 secretion mediated by NLRP3 and AIM2, but not by NLRC4. (**a–k**) ELISA of IL-18 (**a–d, f–k**) and IL-1β (**e**) in peritoneal macrophages primed with LPS for 4 h, followed by stimulation with nigericin for 90 min (**a,d,e,g**), encapsulated flagellin for 6 h (**c**) or infected with *S.* Typhimurium for 6 h (**i**), or unprimed macrophages stimulated with poly(dA:dT) for 3 h (**b,f,h**) or infected with *M. tuberculosis* (**j**) or *L. monocytogenes* (**k**) for 24 h. The indicated kinase inhibitors were added to the cultures 1 h before stimulation or infection for inflammasome activation (**a–c,i–k**). Abbreviations and concentrations of kinase inhibitors are as follows: R406 (R406, 1 μM), Syk inhibitor I (SI, 1 μM), BAY 61-3606 (BAY, 10 μM), PP2 (PP2, 5 μM), SP600125 (SP, 40 μM), TAT-TI-JIP$_{153-163}$ (TAT, 40 μM), SB203580 (SB, 10 μM), FR180204 (FR, 10 μM), and wortmannin (WO, 10 nM). Data are shown as the means ± s.d. of triplicate samples of one experiment. Data shown in **a–f,i–k** are representative of at least three independent experiments and those in **g,h** are representative of two independent experiments. Data were analyzed by one-way ANOVA with Bonferroni multiple comparison test (**a–c,g–k**) or two-tailed unpaired *t* test with Welch's correction (**d–f**). * $P < 0.01$ and ** $P < 0.001$.

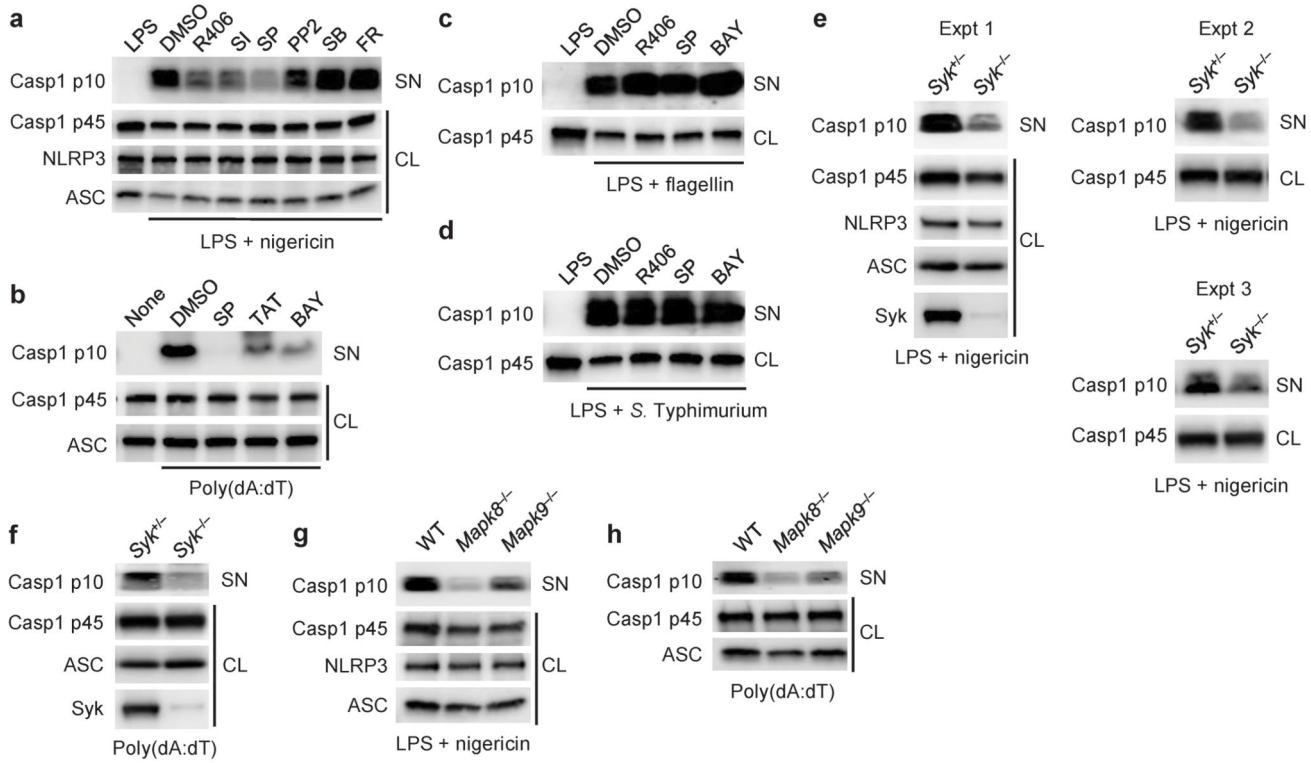

Figure 2.

Involvement of Syk and JNK in NLRP3- and AIM2-mediated caspase-1 activation. (**a–h**) Immunoblotting of inflammasome molecules in peritoneal macrophages primed with LPS for 4 h, followed by stimulation with nigericin for 90 min (**a,e,g**), encapsulated flagellin for 6 h (**c**) or *S.* Typhimurium for 6 h (**d**), or unprimed macrophages stimulated with poly(dA:dT) for 3 h (**b,f,h**). Kinase inhibitors were added to the cultures 1 h before stimulation for inflammasome activation (**a–d**). CL, cell lysates; SN, supernatants. Data shown in **a–f** are representative of at least three independent experiments and those in **g,h** are representative of two independent experiments.

Europe PMC Funders Author Manuscripts

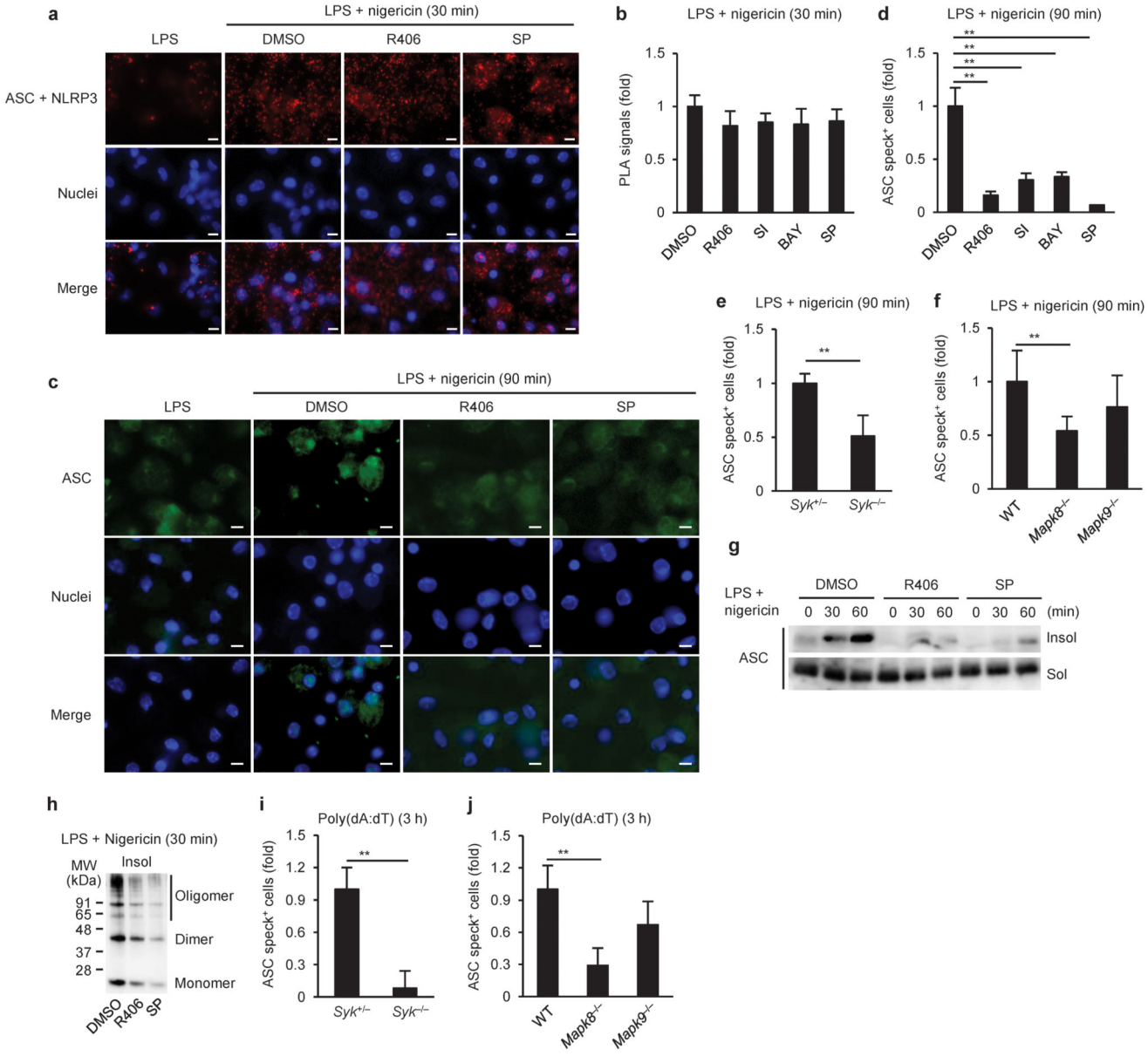

Figure 3.

Requirement of Syk and JNK signals for ASC aggregation. (**a,b**) *In situ* PLA, (**c–f**) ASC staining, or (**g,h**) immunoblotting of ASC in peritoneal macrophages primed with LPS for 4 h, followed by stimulation with nigericin for the indicated time periods in the presence or absence of kinase inhibitors. (**i,j**) ASC staining in unprimed macrophages stimulated with poly(dA:dT) for the indicated time. ASC-NLRP3 complexes are shown in red (**a**), ASC in green (**c**), and nuclei in blue (**a,c**). The number of *in situ* PLA signals per cell was quantified and normalized to that of the solvent control (**b**). The number of ASC speck-positive cell was counted and normalized to that of the solvent control or wild-type (**d–f,i,j**). Triton-soluble (Sol) and -insoluble (Insol) fractions were prepared from the macrophages (**g**), and the Triton-insoluble fraction was treated with DSS (**h**). Data are shown as the means ± s.d.

Europe PMC Funders Author Manuscripts

of triplicate samples of one experiment. Data shown in **a–d,g,h** are representative of at least three independent experiments and those in **e,f,i,j** are representative of two independent experiments. Data were analyzed by Kruskal-Wallis test with Dunn's multiple comparison test (**b,j**), one-way ANOVA with Bonferroni multiple comparison test (**d,f**), two-tailed unpaired *t* test with Welch's correction (**e**) or Mann-Whitney test (**i**). Scale bar, 10 μm. * $P < 0.001$.

Europe PMC Funders Author Manuscripts

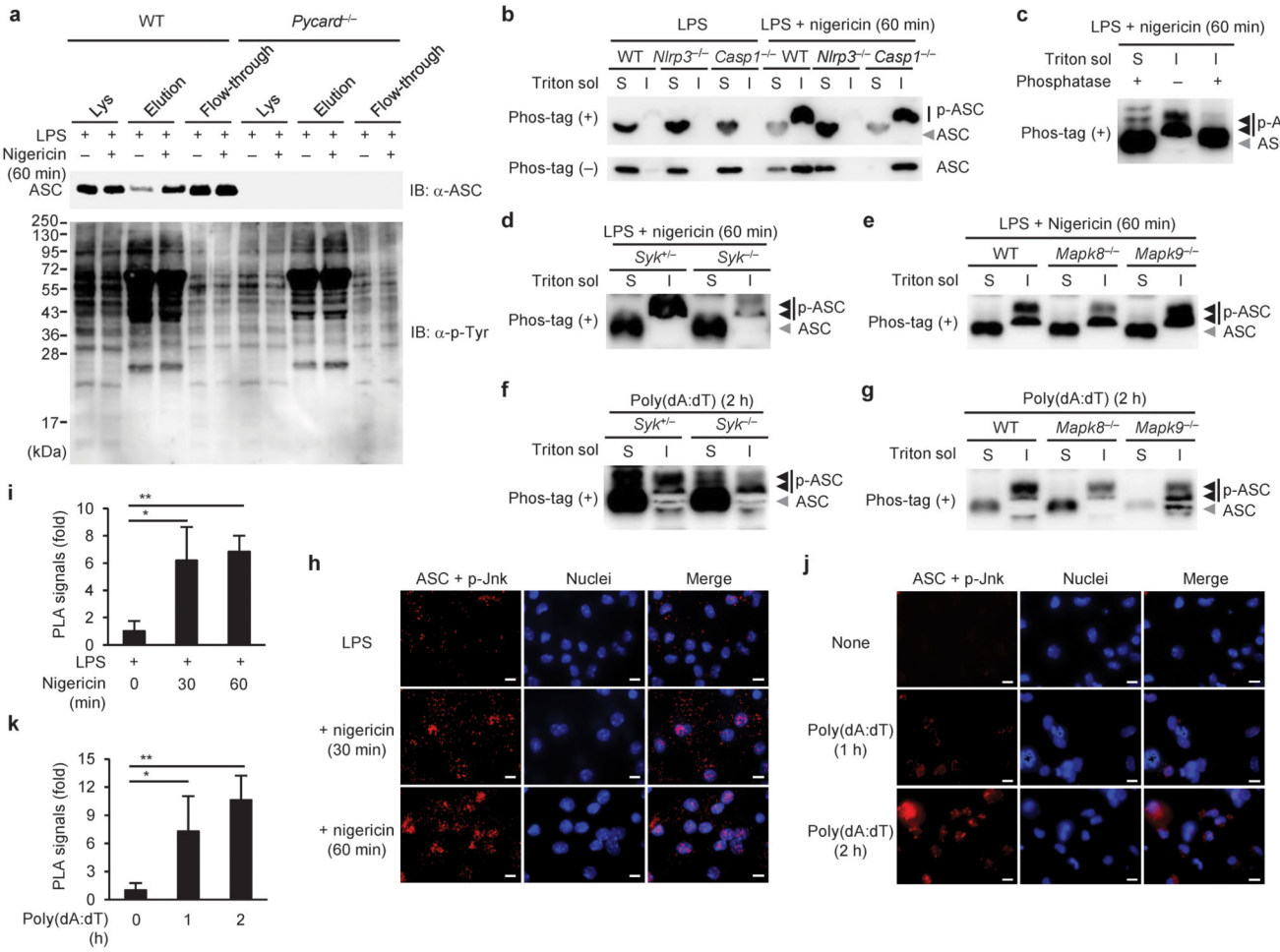

Figure 4.

Phosphorylation of ASC in macrophages upon inflammasome activation. (**a**) Enrichment and detection of phospho-ASC, (**b–e**) Phos-tag MSA, or (**h,i**) *in situ* PLA in peritoneal macrophages primed with LPS for 4 h, followed by stimulation with nigericin for the indicated time periods. (**f,g**) Phos-tag MSA, or (**j,k**) *in situ* PLA in unprimed macrophages stimulated with poly(dA:dT) for the indicated time. Original cell lysates (Lys), elution fraction, and flow-through fraction were prepared by using Pro-Q diamond column (**a**). S and I in **b–g** indicate Triton-soluble and -insoluble fractions, respectively. It should be noted that the Triton-soluble and -insoluble fractions were dissolved in 300 μl and 50 μl of SDS sample buffer, respectively (**b,d–g**). ASC-phospho-JNK complexes and nuclei are shown in red and blue, respectively (**h,j**). The number of *in situ* PLA signals per cell was quantified and normalized to that of the unstimulated control (**i,k**). Data are shown as the means ± s.d. of triplicate samples of one experiment. Data shown in **b,d,h–k** are representative of three independent experiments and those in **a,c,e–g** are representative of two independent experiments. IB, immunoblotting. Data were analyzed by Kruskal-Wallis test with Dunn's multiple comparison test (**i**) or one-way ANOVA with Tukey-Kramer multiple comparison test (**k**). Scale bar, 10 μm. * $P < 0.01$ and ** $P < 0.001$.

Europe PMC Funders Author Manuscripts

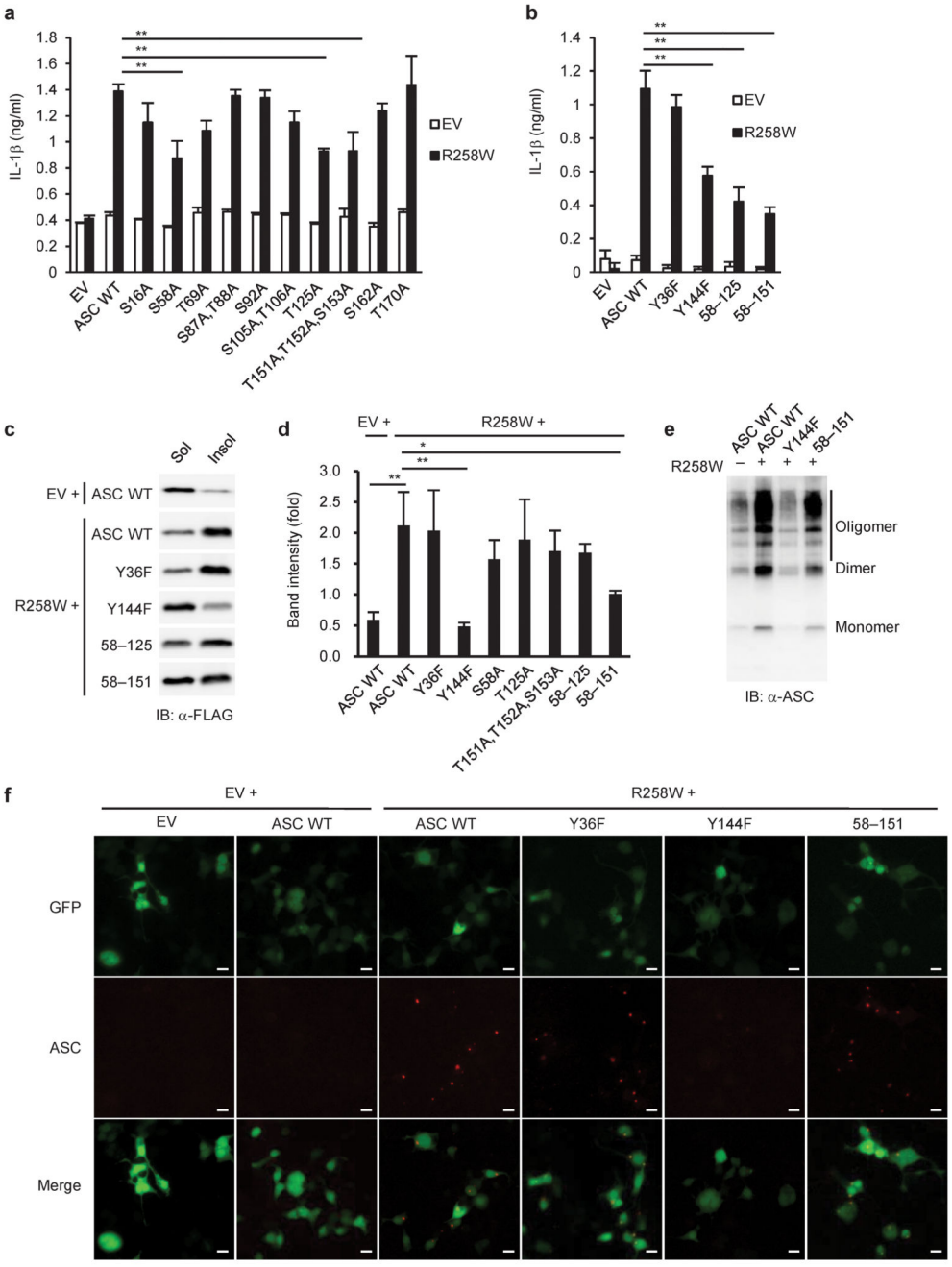

Figure 5.

Identification of amino acid residues in ASC critical for its biological activities. (**a,b**) ELISA of IL-1β in reconstituted HEK293 cells 48 h after co-transfection of pFLAG-ASC (10 ng), pFLAG-NLRP3 (R258W) (100 ng), pro-caspase-1 vector (30 ng) and pro-IL-1β vector (100 ng), or empty vector (EV). (**c–e**) Immunoblotting of ASC or (**f**) ASC staining in reconstituted HEK293 cells 48 h after co-transfection of pFLAG-ASC (50 ng) and pFLAG-NLRP3 (R258W) (100 ng), or EV. The Triton-soluble and -insoluble fractions of the transfected cells were subjected to immunoblotting (**c**), and the ratio of band intensities of

insoluble ASC to soluble ASC was calculated (**d**). The Triton-insoluble fraction was treated with DSS before immunoblotting (**e**). ASC is shown in red, and pmax-GFP (100 ng) was used to visualize transfected cells (green) (**f**). Data are shown as the means ± s.d. of triplicate samples of one experiment representative of three independent experiments. IB, immunoblotting; 58–125, ASC (S58A,T125A); 58–151, ASC (S58A,T151A,T152A,S153A). Data were analyzed by one-way ANOVA with Bonferroni (**a,b**) or Tukey-Kramer multiple comparison test (**d**). Scale bar, 10 μm. * $P < 0.05$ and ** $P < 0.001$.

Europe PMC Funders Author Manuscripts

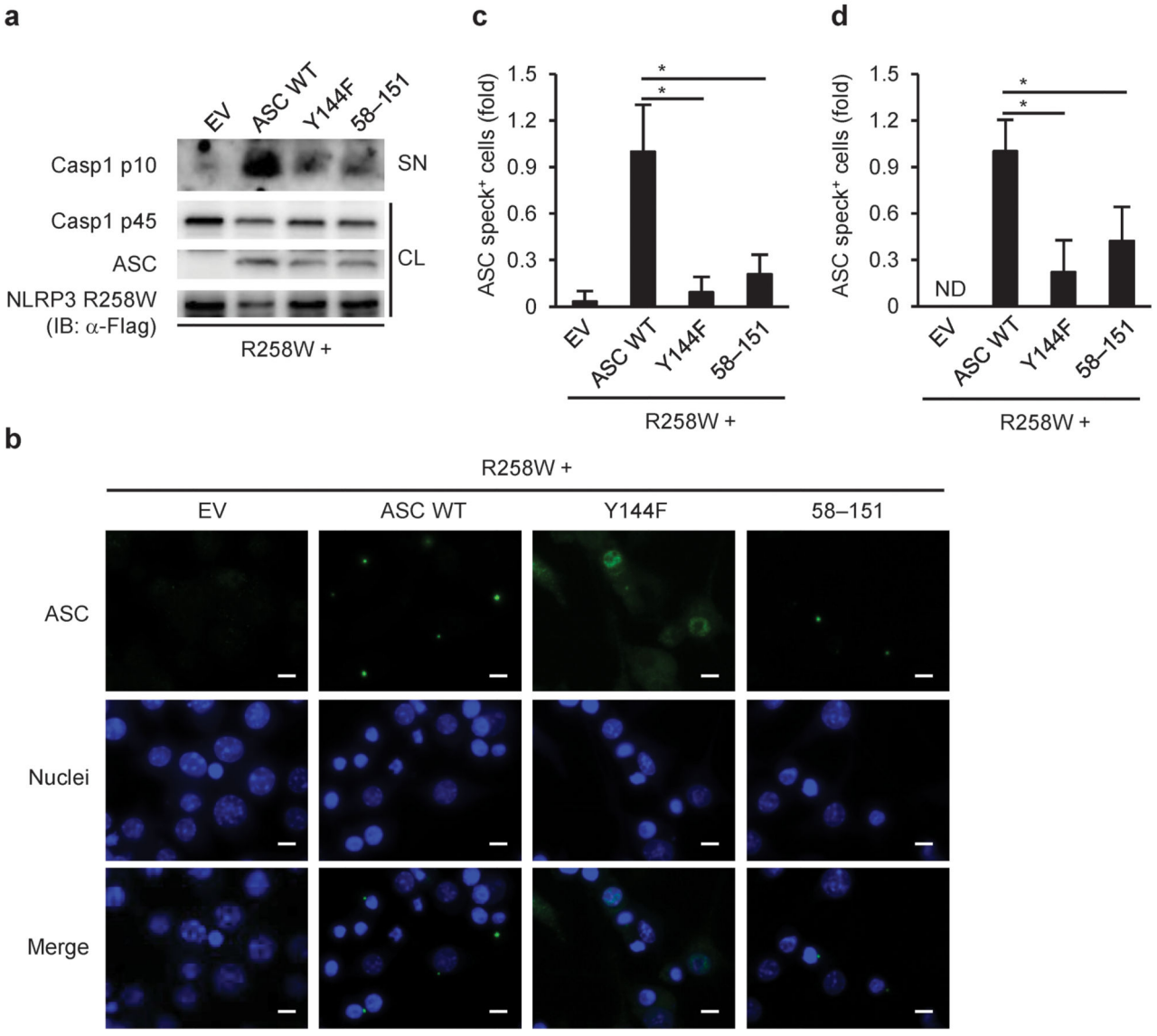

Figure 6.

Critical roles of the possible phosphorylation sites of ASC in macrophages. (**a**) Immunoblotting of inflammasome molecules or (**b,c**) ASC staining in reconstituted RAW264.7 cells 9 h after co-transfection of pFLAG-ASC and pFLAG-NLRP3 (R258W), or empty vector (EV). (**d**) ASC staining in reconstituted primary *Pycard*$^{-/-}$ peritoneal macrophages 9 h after co-transfection of pFLAG-ASC and pFLAG-NLRP3 (R258W). ASC is shown in green, nuclei in blue (**b**). The number of ASC speck-positive cell was counted and normalized to that of the cells transfected with EV (**c,d**). CL, cell lysates; SN, supernatants; ND, not detected. Data are shown as the means ± s.d. of triplicate samples of one experiment representative of three independent experiments. Data were analyzed by one-way ANOVA with Bonferroni multiple comparison test (**c,d**). Scale bar, 10 μm. * $P <$ 0.001.

Europe PMC Funders Author Manuscripts

Europe PMC Funders Author Manuscripts

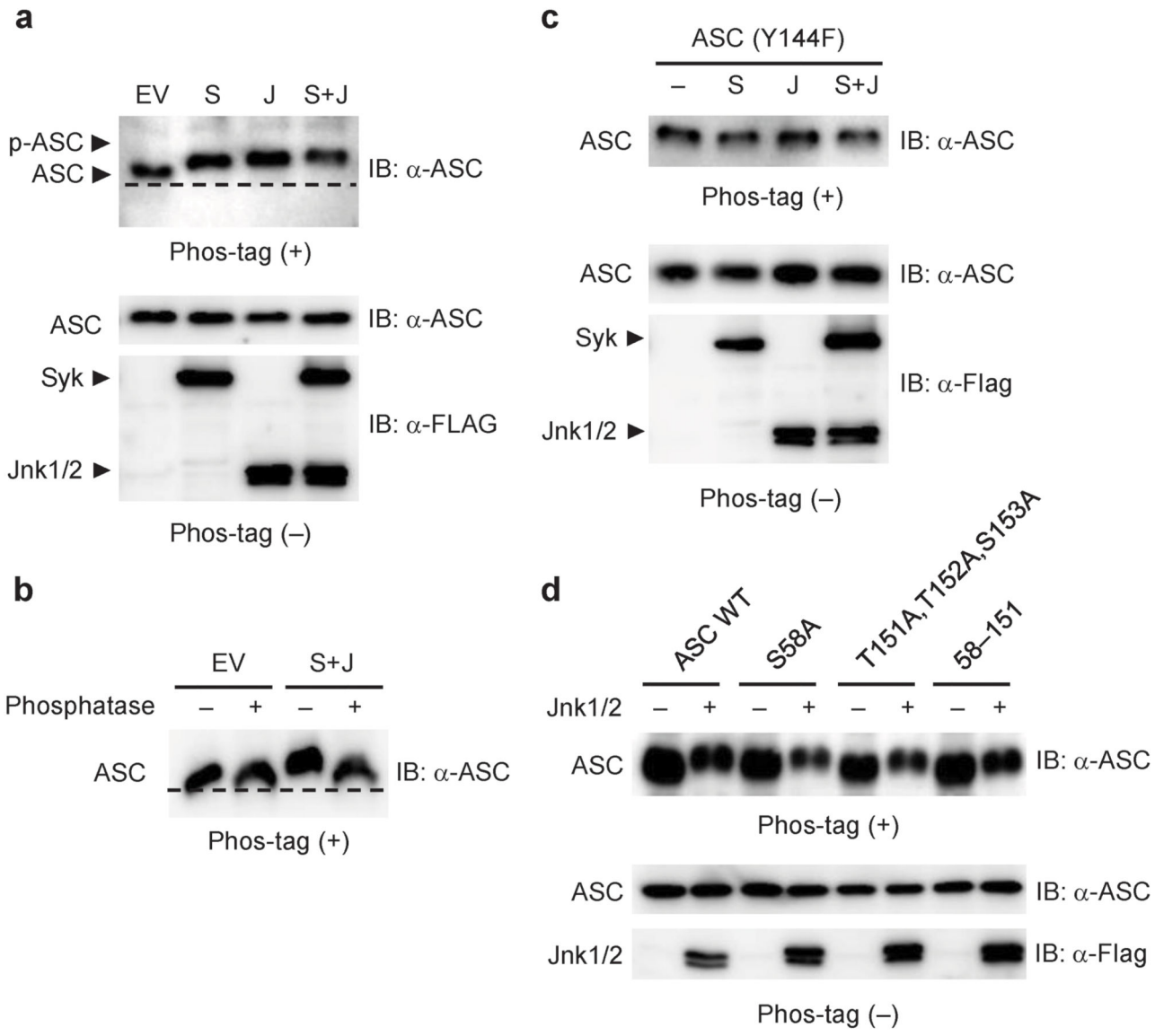

Figure 7.

Identification of phosphorylation sites in ASC. (**a–d**) Phos-tag MSA in reconstituted HEK293 cells 48 h after co-transfection of pFLAG-ASC (50 ng), pFLAG-Syk (300 ng), pFLAG-JNK1 (300 ng) and pFLAG-JNK2 (300 ng), or empty vector (EV). The lanes indicated as S, J, and S + J refer to transfection with pFLAG-Syk, with both pFLAG-JNK1 and pFLAG-JNK2, and with these three vectors, respectively. IB, immunoblotting. Data are representative of three independent experiments.

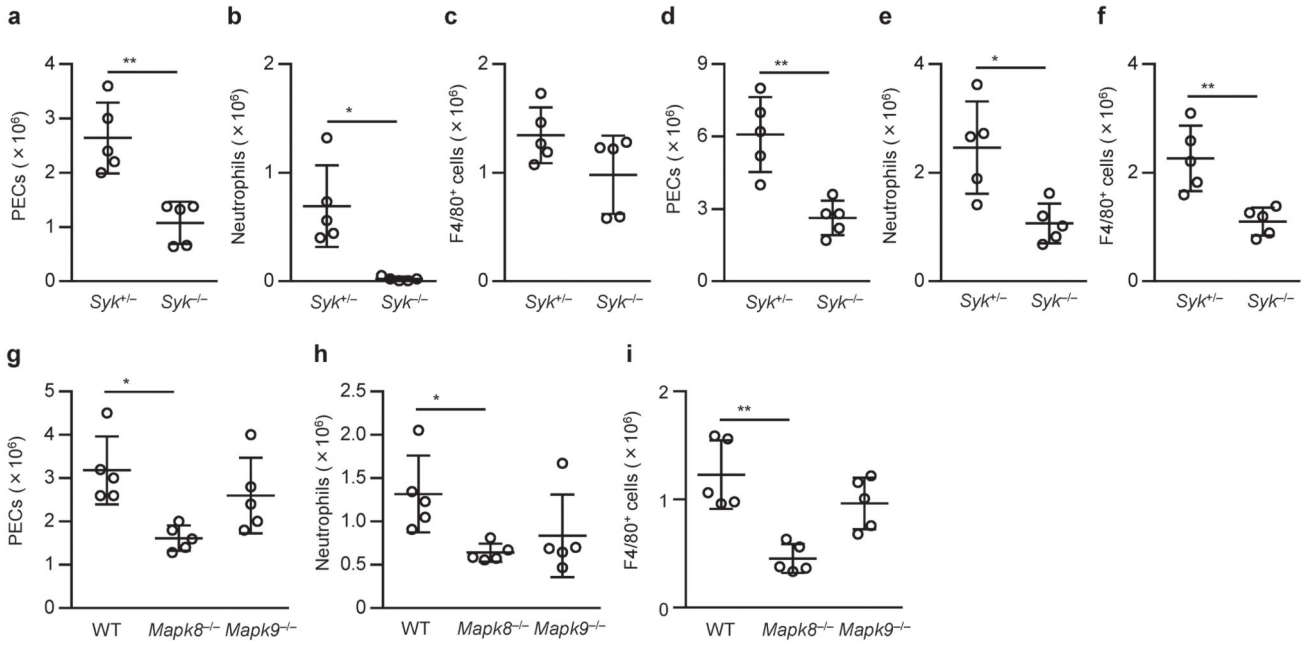

Figure 8.

Involvement of Syk and JNK in inflammatory responses to MSU *in vivo*. (**a–i**) Infiltration of inflammatory cells in the peritoneal cavity of chimeric mice induced by intraperitoneal injection of MSU (**a–c,g–i**) or alum (**d–f**) 6 h after injection. Absolute numbers of peritoneal exudate cells (PECs) (**a,d,g**), Gr-1$^+$ F4/80$^-$ neutrophils (**b,e,h**), and F4/80$^+$ monocytes and macrophages (**c,f,i**) in the peritoneum were then determined. Data are shown as dots, and the bars indicate the means ± s.d. (n = 5). Data were analyzed by two-tailed unpaired Mann-Whitney test (**a,c**), two-tailed unpaired *t* test with Welch's correction (**b,d–f**), one-way ANOVA with Bonferroni multiple comparison test (**g**) or Kruskal-Wallis test with Dunn's multiple comparison test (**h,i**). * $P < 0.05$ and ** $P < 0.01$.

Europe PMC Funders Author Manuscripts